Advanced Composite Materials, 2024
Vol. 00, No. 00, 1–15, https://doi.org/10.1080/09243046.2024.2351667

Taylor & Francis
Taylor & Francis Group

Check for updates

A stochastic modelling framework for predicting flexural properties of ultra-thin randomly oriented strands

Xiaodong Xu [a], André Jesus [b], Yi Wan[c] and Jun Takahashi[c]

[a]*Centre for Aeronautics, School of Aerospace, Transport and Manufacturing, Cranfield University, Cranfield, UK;* [b]*School of Architecture, Building and Civil Engineering, Loughborough University LE11 3TU, Leicestershire, UK;* [c]*Department of Systems Innovation, School of Engineering, The University of Tokyo, 113-8656, Bunkyo ku, Tokyo, Japan*

(*Received 7 February 2024; accepted 1 May 2024*)

A stochastic modelling framework is developed to predict the flexural properties of high-strength sheet moulding compounds made of randomly oriented ultra-thin carbon fibre-reinforced thermoplastic prepreg tapes. The model enables reliable designs using ultra-thin randomly oriented strands with less testing, leading to potential applications in automotive primary structures. The stochastic model is based on a Monte Carlo simulation. The flexural modulus is predicted using classical laminate theory, while the flexural strength is predicted by following a Weibull distribution. Fibre discontinuities are considered through stress concentrations introduced by tape overlaps. The results are validated against new 3-point bending and previously reported 4-point bending experimental results. A scaling effect on strength and scatter is predicted, and its implications for structural applications are also discussed.

Keywords: strength; moulding compounds; thin ply; thermoplastics; randomly oriented strands

1. Introduction

Carbon fibre reinforced thermoplastic composites have been increasingly used in the automotive industry [1]. They have excellent material properties, light weight, and recyclability. There are different manufacturing methods for thermoplastic composites such as injection moulding and compression moulding. Compression moulding can produce relatively complex parts, and the process is more energy efficient compared to other methods such as injection moulding [2]. When compression moulded into sheet moulding compounds, Randomly Oriented Strands (ROS) of thermoplastic prepreg tapes can achieve a high fibre volume fraction and good formability. Despite the attractive benefits, ROS generally have low strength [3].

The existing modelling methods for ROS have been reviewed by Visweswaraiah et al. [3]. According to Li et al. [4], the local variability in the microstructure must be considered to accurately predict their strength. The models which can represent the internal structure of ROS

Corresponding author. Xiaodong Xu Email: xiaodong.xu@cranfield.ac.uk;
André Jesus Email: A.Jesus@lboro.ac.uk

© 2024 The Author(s). Published by Informa UK Limited, trading as Taylor & Francis Group.
This is an Open Access article distributed under the terms of the Creative Commons Attribution-NonCommercial-NoDerivatives License (http://creativecommons.org/licenses/by-nc-nd/4.0/), which permits non-commercial re-use, distribution, and reproduction in any medium, provided the original work is properly cited, and is not altered, transformed, or built upon in any way. The terms on which this article has been published allow the posting of the Accepted Manuscript in a repository by the author(s) or with their consent.

were therefore developed for failure predictions. For example, Harper et al. [5] developed a geometrical modelling scheme to produce representative architectures for ROS. Based on the scheme, they used a multi-scale Finite Element (FE) model to accurately predict the tensile properties of ROS. Kravchenko et al. [6] developed a detailed FE model for the prediction of tensile properties of stochastic Prepreg Platelet Moulded Composites (PPMC). The model can capture non-linearity of this type of ROS material under tension and more recently under bending [7]. Shah et al. [8] developed a validated FE modelling strategy which captures many of the realistic features of both thermoset and thermoplastic ROS. These models were focused on the performance of the ROS made from prepregs of typical thickness.

Recently, ultra-thin ROS of both thermoplastic [9] and thermoset [10] prepregs with a thickness of less than 100 microns have shown much improved mechanical properties. This is partially due to ultra-thin prepregs' matrix cracking and delamination suppression characteristics [11]. The thermoplastic Ultra-thin ROS made of prepregs with a thickness of 44 microns, referred to as UT-ROS in this paper, shows doubled tensile strength compared to some existing ROS. UT-ROS consistently exhibited fibre-dominant failures under tension [12] and bending [13]. However, the random nature of ROS leads to large variation in their properties, hence there is an urgent need for developing models that can address reliability issues which overcome limitation of deterministic models.

Different models have also been developed for the thermoplastic UT-ROS such as analytical models [14,15] stochastic models [16,17] and Peridynamic models [18]. A stochastic modelling framework was also established to predict the tensile behaviour of UT-ROS by Jesus and Xu [17]. The tensile properties such as Young's modulus and tensile strength were predicted within 6.3%. Compared to the other models [15,16,18], this model captured the morphology of the individual tapes, so can explain the failure mechanism from the internal structure such as tape overlaps.

The key to its capability of strength prediction [17] is the adoption of Weibull theory [19] to UT-ROS materials. It assumes that when the weakest point in the chain breaks, the entire chain will fail. It is suitable for predicting the failure of quasi-brittle materials like UT-ROS. Weibull theory has been successfully used to predict fibre failures in continuous fibre composites [20–24] and discontinuous fibre composites [17,25]. However, it should not be confused with the other 'weakest-link' methods e.g. applied by Selezneva et al. [26] which seeks to find a failure path in the ROS that fail more gradually.

Tape lengths were found to influence the strength of ROS by Yamashita et al. [12] and by Sattar et al. [7]. Longer tape lengths led to higher tensile strengths in UT-ROS [12], but the trend is less clear for conventional ROS [7]. For UT-ROS under tension, it was successfully predicted by Jesus and Xu [17] but has not been reported under bending or predicted by the existing models e.g. by Qu et al. [18].

In this paper, a modelling framework is developed to predict the brittle flexural properties of thermoplastic UT-ROS materials. Specifically, the flexural modulus is predicted using a Monte Carlo simulation and Classical Laminate Theory (CLT). The flexural strength is predicted using Weibull theory. Fibre discontinuities are addressed via stress concentrations caused by tape overlaps. The modelling results are carefully validated by a wide range of flexural experiments including new results with different tape lengths under 3-point bending. The modelling framework successfully captures the difference between 4-point and 3-point bending results, and the effect of tape lengths under 3-point bending.

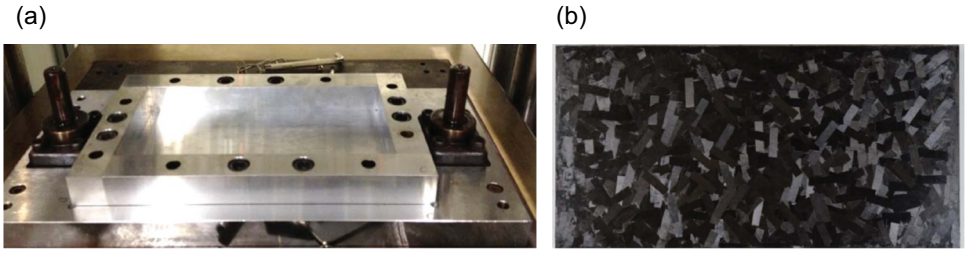


Figure 1. UT-ROS manufacture (a) mould, (b) moulded plate with 18 × 5 mm tapes.

2. Experiments

2.1. *Material properties*

The thermoplastic prepreg used is TR 50S carbon fibre tows (Mitsubishi Chemical Co., Japan) spread to form ultra-thin 44 microns sheets impregnated with DIAMIRON™ C polyamide-6 resin (Mitsubishi Chemical Co., Japan). The chopped prepreg tapes were processed by compression moulding using the mould as shown in Figure 1a. The volume fraction of the prepreg is 55%. The moulding conditions are 250°C and 5 MPa pressure for 10 min. The moulded UT-ROS plate has a dimension of 250 × 125 mm as shown in Figure 1b. After trimming 5 mm off all edges, the plate was cut into six flexural specimens per case using a wet diamond saw (MARUTO Testing Machine Co., Japan).

2.2. *Flexural tests*

Two sets of flexural tests were conducted to validate the models. Six specimens have a dimension of 125 × 30 × 3 mm and were tested on a 3-point bending fixture with a span of 80 mm (Figure 2a). Previously, six 125 × 35 × 3.1 mm specimens were tested on a 4-point bending jig with a lower span of 96 mm and an upper span of 48 mm [13] (Figure 2b). All specimens exhibited fibre-dominant first failure at the tension side as captured by a high-speed camera in Figure 2c and d. This is the same failure mode as that under tension [12], so the modelling framework [17] for tension can be further developed for bending.

3. Modelling framework

The current stochastic modelling framework is developed using MATLAB (MathWorks, US). Weibull theory is introduced for tape fracture, considering stress concentrations caused by tape overlaps. The modelling framework is focused on the prediction of brittle failure in the current UT-ROS. Tape debonding is not predicted since both ultra-thin prepreg and tough thermoplastic resin manage to suppression of sub-critical damage in accordance with the experimental observations [27].

A total of 10 tape configurations are randomly generated and statistical features are subsequently extracted from them. A flowchart of the modelling framework is presented in Figure 3. It consists of three steps: (1) Initialisation; (2) Matrices assembly; (3) Failure prediction.

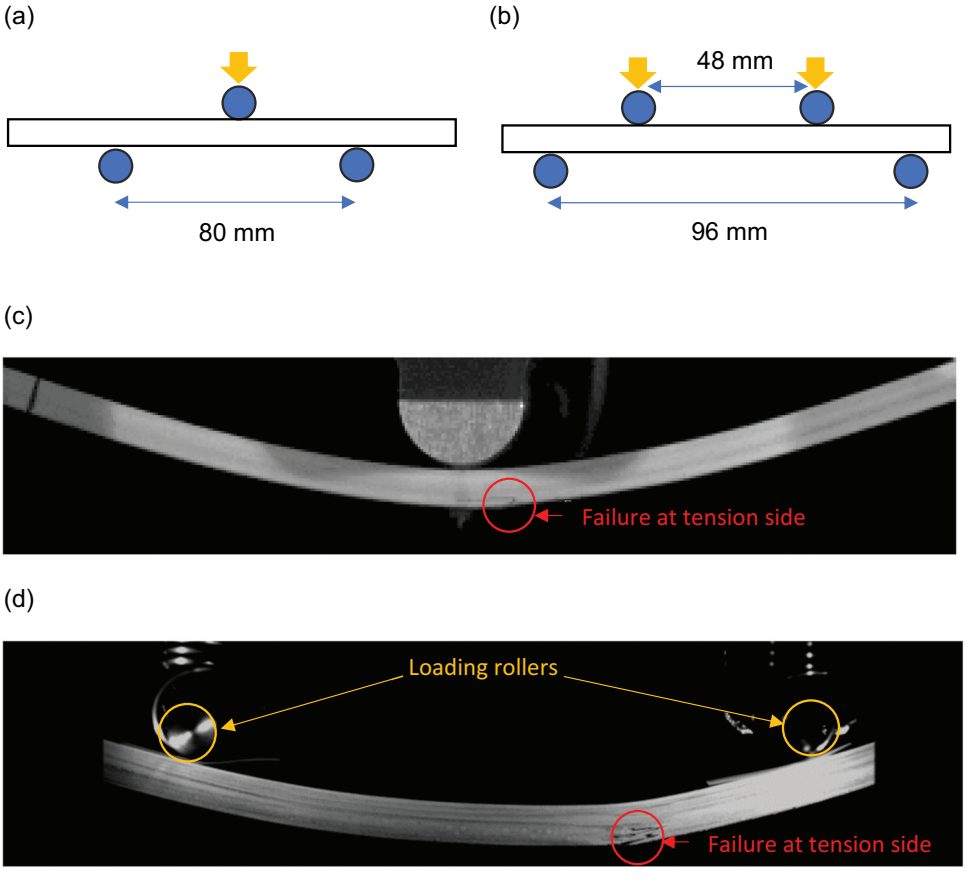


Figure 2. Flexural tests under (a) 3-point bending, (b) 4-point bending, (c) a picture showing fibre-dominant tensile first failure under 3-point bending, and (d) under 4-point bending.

3.1. *Model set-up*

During initialization, the tapes' material and geometrical properties are read. The tapes are placed into different layers through the thickness. Each layer is 44-micron thick, same as the tape thickness, so there are 70 layers for a typical 3.1 mm-thick specimen. The model thickness is the same as the average laminate thickness. The total tape number in the model is determined according to weight conservation. The distribution of the tapes is assigned as a uniform distribution from which random scalar values are drawn for each of the coordinates of the moulding area and the rotation angle. Under 4-point bending, the moulding area is a 50 × 35 mm rectangle. It is offset by the length of one tape from the boundary of the laminate for the 4-point bending case, as displayed in Figure 4a. This is approximately in accordance with the upper span of the 4-point bending jig and the specimen width within which the bending moment is constant. The angle of the tapes is defined as shown in Figure 4b, with the 0º being the longitudinal direction of the specimen (X-direction). Under 3-point bending, the moulding area is changed to 25 × 30 mm. This is to reflect the narrow specimens used and a non-uniform bending moment distribution under 3-point bending. A smaller volume of material is under

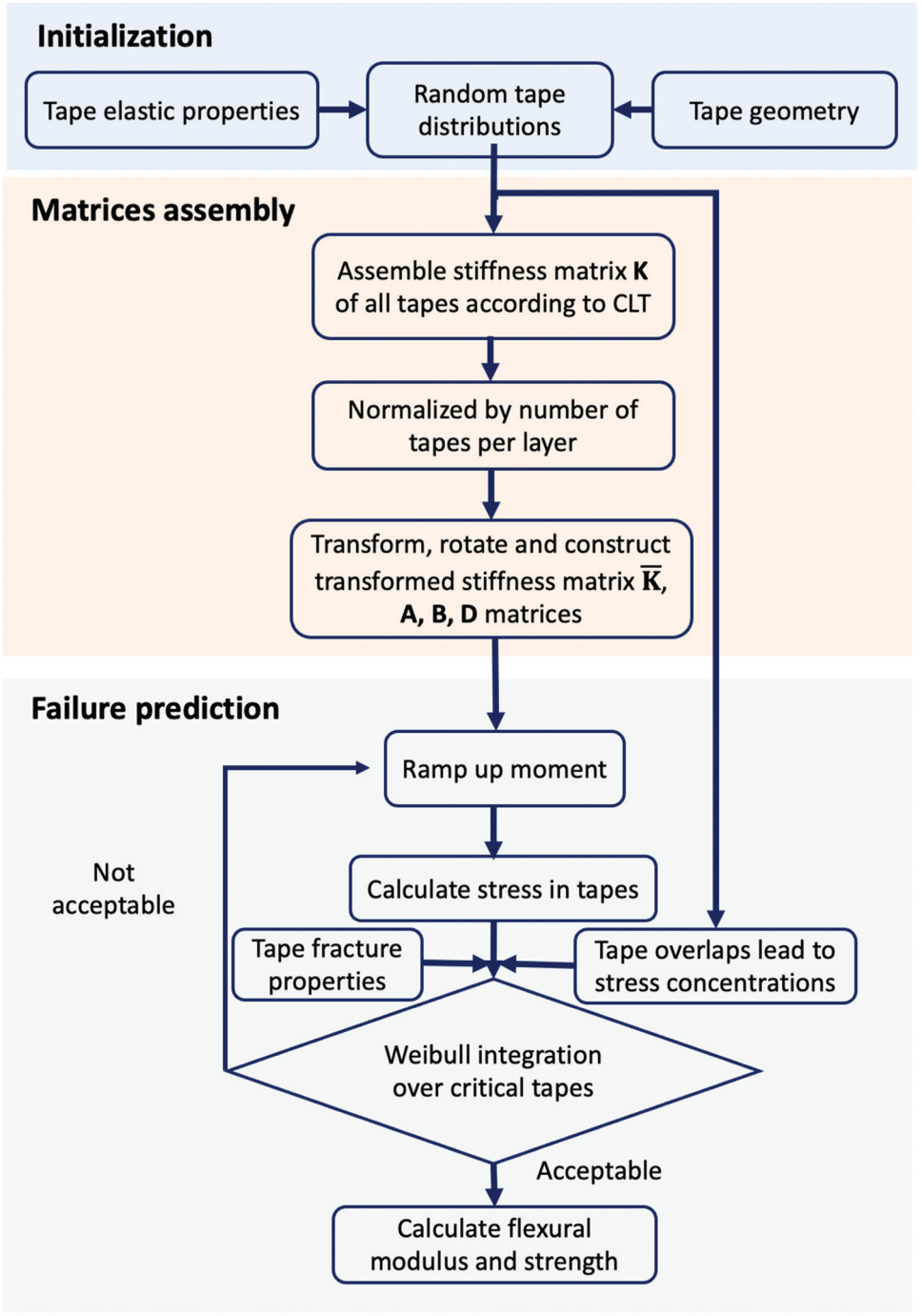


Figure 3. Flowchart of the modelling framework.

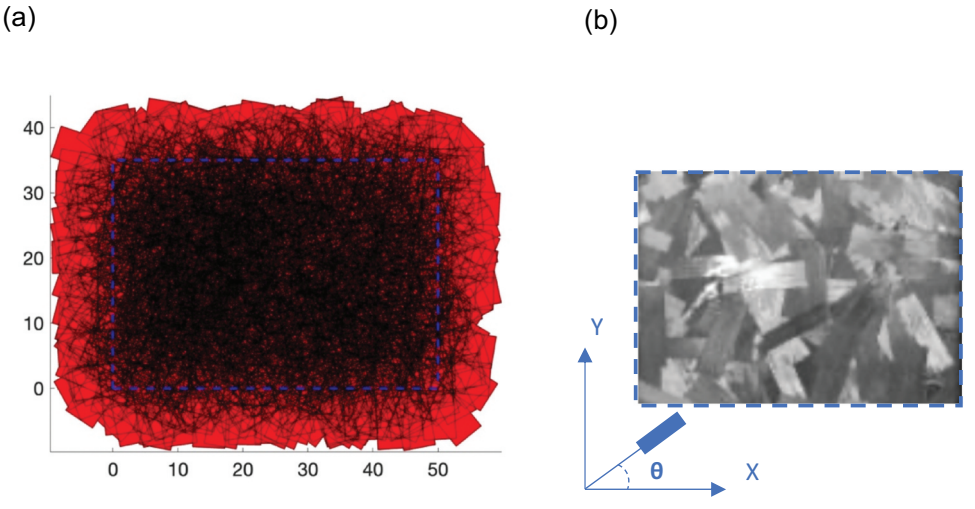


Figure 4. A laminate consists of randomly oriented tapes with (a) a blue boxing indicating the modelled region, (b) angle of the tapes defined with the actual specimen.

high bending stress compared to 4-point bending. A parametric study is done to compare results with different gauge lengths later.

The second step is to assemble matrices. The elastic properties of the UT-ROS are determined according to CLT, same as the process under tensile loading [17]. This includes the assembly of stiffness matrix $\boldsymbol{K}$, normalisation by the tapes per layer of 44 microns, transformation and rotation to form transformed stiffness matrix $\overline{\boldsymbol{K}}$.

$$\boldsymbol{K} = \frac{1}{1 - v_{12}v_{21}} \begin{bmatrix} E_{11} & v_{21}E_{11} & 0 \\ v_{12}E_{22} & E_{22} & 0 \\ 0 & 0 & G_{12}(1 - v_{12}v_{21}) \end{bmatrix} \tag{1}$$

where the material elastic properties are listed in Table 1.

Table 1. Tape geometrical and material properties [13,17].

Geometrical Property	Value
Critical tape angle [°]	0–10
Tape width [mm]	5
Tape length [mm]	19 (4-point); 6, 12, 18, 24 (3-point)
Tape thickness [mm]	0.044
Tape volume fraction [%]	55
Material Property	**Value**
E_1 [GPa]	105
E_2 [GPa]	4
G_{12} [GPa]	1.2
V_{12}	0.3
V_{21}	0.01

The transformed elastic matrix $\bar{K}$ is computed by successive axes rotation and addition of the contribution from each individual tape according to Equation (2).

$$\overline{\boldsymbol{K}} = \boldsymbol{T}^{-1}\boldsymbol{K}\boldsymbol{R}\boldsymbol{T}\boldsymbol{R}^{-1} \tag{2}$$

where $\boldsymbol{T}$ is the transformation matrix and $\boldsymbol{R}$ is the Reuter's matrix.

The sum of transformed elastic matrix of all the tapes in each 'layer' is calculated and normalised by the number of tapes in each 'layer' to account for the average effect of randomly oriented tapes within the same 'layer'.

$$\overline{\boldsymbol{K}}_{\boldsymbol{n}} = \frac{1}{N_{tpl}}\sum_{i=1}^{N_{tpl}} \boldsymbol{T}^{-1}\boldsymbol{K}\boldsymbol{R}\boldsymbol{T}\boldsymbol{R}^{-1} \tag{3}$$

where $\bar{K}_n$ is the normalised stiffness matrix in each 'layer'. N_{tpl} is the number of tapes per 'layer'.

$\boldsymbol{A}$, $\boldsymbol{B}$ and $\boldsymbol{D}$ matrices are then directly related with the normalized stiffness matrix $\bar{K}_n$ according to Equations 4-6.

$$\boldsymbol{A} = \sum_{\boldsymbol{k}=1}^{\boldsymbol{N_l}} \overline{\boldsymbol{K}}_{\boldsymbol{n}}(z_{k+1} - z_k) \tag{4}$$

$$\boldsymbol{B} = \frac{1}{2}\sum_{\boldsymbol{k}=1}^{\boldsymbol{N_l}} \overline{\boldsymbol{K}}_{\boldsymbol{n}}\left(z_{k+1}^2 - z_k^2\right) \tag{5}$$

$$\boldsymbol{D} = \frac{1}{3}\sum_{\boldsymbol{k}=1}^{\boldsymbol{N_l}} \overline{\boldsymbol{K}}_{\boldsymbol{n}}\left(z_{k+1}^3 - z_k^3\right) \tag{6}$$

where N_l is the total number of layers, z_k is the distance from the laminate mid-plane to the bottom of each layer k.

Finally, failure prediction is conducted based on the stress from CLT, tape overlaps and Weibull theory. A moment $\boldsymbol{M}$ per unit width is ramped up and applied to the modelled region, so its mid-plane strain ε and curvature κ can be calculated.

$$\begin{Bmatrix} 0 \\ \boldsymbol{M} \end{Bmatrix} = \begin{bmatrix} \boldsymbol{A} & \boldsymbol{B} \\ \boldsymbol{B} & \boldsymbol{D} \end{bmatrix} \begin{Bmatrix} \varepsilon \\ \kappa \end{Bmatrix} \tag{7}$$

where $\boldsymbol{A}$, $\boldsymbol{B}$ and $\boldsymbol{D}$ are the extensional, coupling and bending matrices, respectively.

The mid-plane strain ε and curvature κ are then converted into the fibre-direction stress of the chopped tapes, σ_u, according to Equation (8) in which z is the location of the 'layer' where the tapes are located.-

$$\sigma_u = \overline{\boldsymbol{K}}\varepsilon + z\overline{\boldsymbol{K}}\kappa \tag{8}$$

The elastic flexural modulus, E_B, is from $\boldsymbol{D}$ matrix according to Equation (9). E_B is compared against the experimental result [5].

$$E_B = 12D_{11}/l_t^3 \tag{9}$$

The moment $\boldsymbol{M}$ is translated into an equivalent flexural stress σ_B, via Equation (10) in which l_t is the laminate thickness. σ_B at failure will be compared against the experimental results.-

$$\sigma_B = 6M/l_t^2 \tag{10}$$

3.2. *Weibull theory*

In the previous work [22], Weibull theory was adopted to predict fibre failure in continuous fibre composites. It was transformed into a failure criterion for discontinuous UT-ROS [17] as a function of both the volume and the stress of tapes in Equation (11). This is appropriate for thermoplastic UT-ROS material because its failure is fibre-dominated. This is a result of their tough matrix and thin plies, both of which prohibit matrix failure.

$$\sum_{i=1}^{\text{Number of critical tapes}} V_i\left(\sigma_{c,i}/\sigma_{\text{unit}}\right)^m = 1 \tag{11}$$

where $\sigma_{c,i}$ is the updated fibre-direction tensile stress in the critical tapes, V_i is the volume of the critical tapes, σ_{unit} is the tensile strength of a unit volume of material and m is the Weibull modulus. The fibre failure parameters are assumed as $\sigma_{\text{unit}} = 3131$ MPa and $m = 41$, based on data of similar fibres [22].

The tapes with shallow angles are identified Figure 5a. They are referred to as critical tapes which have high stress in the fibre direction, so are most likely to fail. According to Katsivalis et al. [10], the failure mode of ROS changes from tape fracture to tape pull-out between 10° and 20°. Since UT-ROS consistently exhibit tape fracture rather than tape

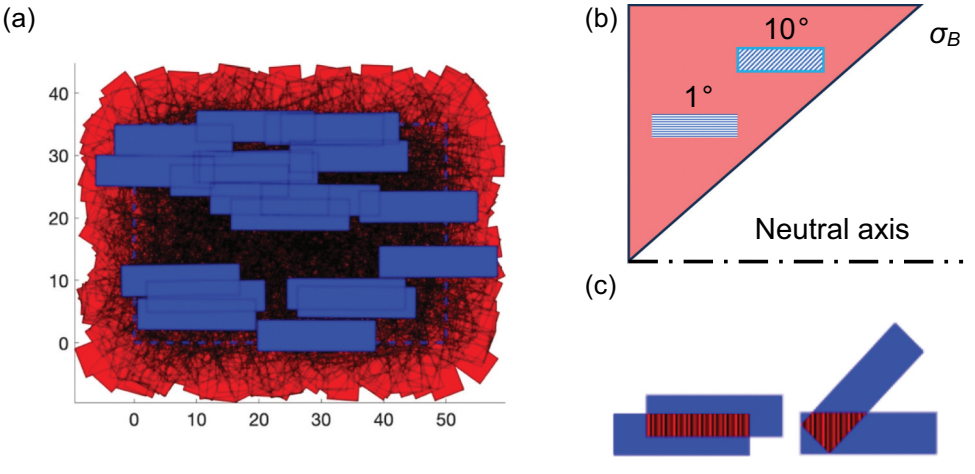


Figure 5. Critical tapes (a) marked in blue in plane, (b) through depth, and (c) their overlapped area with other tapes.

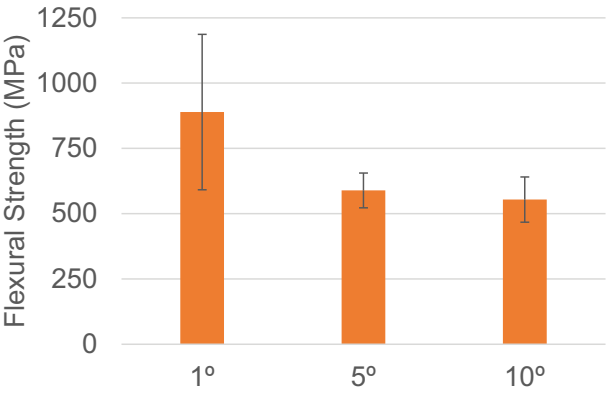


Figure 6. Predicted flexural strength converges with different maximum critical tape angles.

pull-out, the critical tapes are defined as 10°or less in this work. Because of the stress gradian through thickness under bending, the stress in the smallest angled tapes (e.g. 1° or less) may not be the greatest like under tension [17] if they are not near the surface as shown in Figure 5b. It is therefore necessary to broaden the range of the critical tapes to generate more accurate results under bending. A parametric study was also conducted to investigate the influence of the angles of the critical tapes on flexural strength. The maximum angle varies from 1° to 10°. The predict flexural strength is not very sensitive to the angle of the critical tapes from 5° to 10° as shown in Figure 6.

It is important to address discontinuities in UT-ROS. It was done by assuming that the critical tapes carry extra force from the other angled tapes which interact with them in each layer [17]. This leads to an increase of stress in the critical tapes via a Stress Concentration Factor (SCF) which is defined in Equation (12).

$$SCF = \frac{\sigma_c + \sigma_a}{\sigma_c} \tag{12}$$

where σ_a is from the shared force according to the total force in the angled tape and the overlapped area in Figure 5c, and then divided by the tape width and length [17]. σ_c is the fibre-direction stress from CLT which does not consider force sharing.

For the critical tapes, their fibre-direction stress, σ_c, is multiplied by the SCF. The updated fibre-direction stress, $\sigma_{c,\,i,}$ is added to the Weibull integral according to Equation (11). Once failure is deemed to occur at a certain moment, the flexural strength σ_B is determined.

4. Results comparison

The measured load–displacement response under bending is fairly linear except around the peak load. The observed slight nonlinearity could be due to plasticity in the resin. The proposed model however ignores any material nonlinearity for simplicity.

In Figure 7, the modelling results are compared against the 4-point bending experimental results [13]. The predicted average flexural modulus is 2.0% higher and the

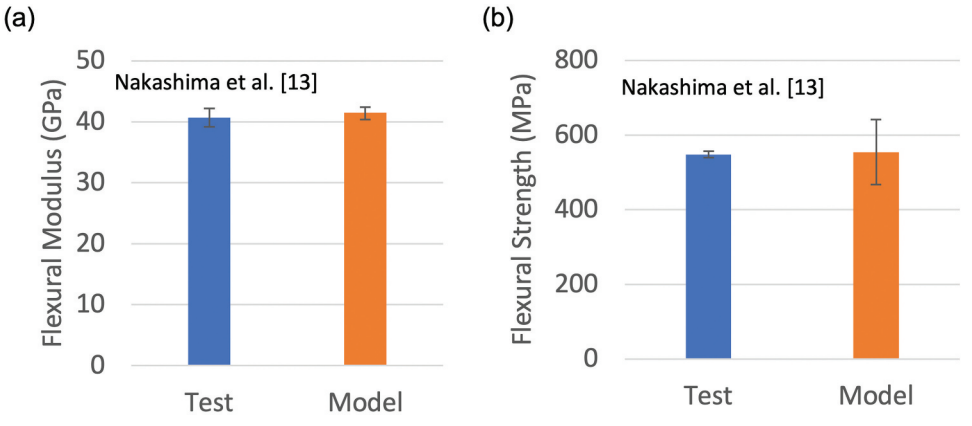


Figure 7. Results comparison between 4-point bending tests and the model for (a) flexural modulus, and (b) flexural strength.

predicted average flexural strength is 1.1% higher than the experimental results. The predicted scatter for flexural modulus is very similar to the measured scatter [13], but the predicted scatter for flexural strength is larger than the measured value [13].

The modelling approach needs to be tailored to predict the 3-point bending results. This is because the current modelling framework assumes a constant moment in the gauge section, which is not true in 3-point bending experiments. An appropriate gauge length of the model needs to be assumed to reflect the reduced stressed volume under 3-point bending. A parametric study is performed by changing the model gauge length from 50, 37.5 to 25 mm as shown in Figure 8. It was found that the 25 mm gauge length yields satisfactory results (within 3.7%). A shorter modelled gauge length may not be suitable as too many tapes with a length of 18 mm would partially fall outside the modelled area. To capture true non-uniform bending stress distribution under 3-point bending, a FE model is needed, which is beyond the scope of the current work.

A 25×30 mm gauge area is therefore chosen for 3-point bending models from now on. The predicted flexural strength is within 3.7% of the new 3-point bending test results

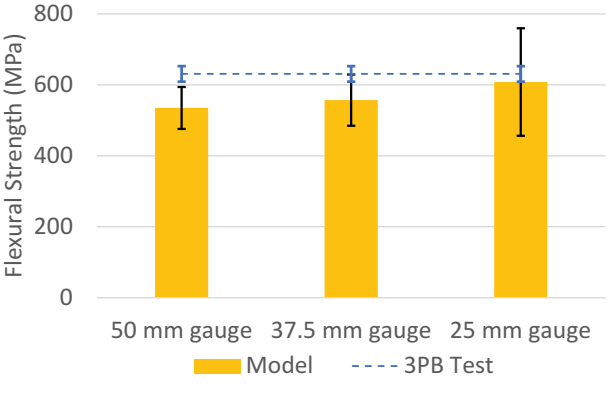


Figure 8. Comparison of modelling results of different model gauge lengths and the 3-point bending experimental results.

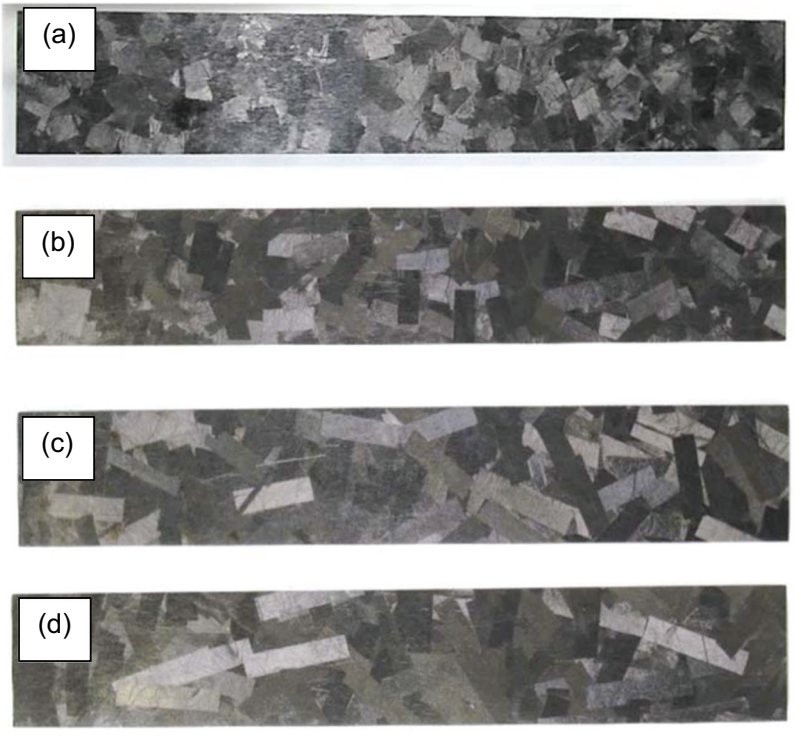


Figure 9. Flexural specimens with different tape lengths of (a) 6 mm, (b) 12 mm, (c) 18 mm, and (d) 24 mm.

in Figure 8. Since the volume of material under high moment is larger under 4-point bending [13] than 3-point, the measured 4-point flexural strength (Figure 7) is lower than 3-point (Figure 8) according to the Weibull theory. This difference has been successfully captured by the current modelling framework.

New 3-point bending specimens were made with different tape lengths, ranging from 6, 12, 18 to 24 mm as shown in Figure 9. This provides an extra validation case for the current modelling framework. The predictions show a gradual increase of average flexural strength with longer tapes which agree well with the experimental results as seen in Figure 10. The predicted average strength is within 12.5% of the experimental results, but the predicted scatter is larger than the experimental scatter.

5. Discussion

The modelled gauge length is further increased to 75 mm and 100 mm as shown in Figure 11. When the gauge length increases with a fixed gauge width of 30 mm, the modelled moulding area also increases. This leads to a lower predicted flexural strength because of the larger stressed volume, which can be explained by Equation (11) or Weibull theory. This implies that large composite structures made of UT-ROS may be

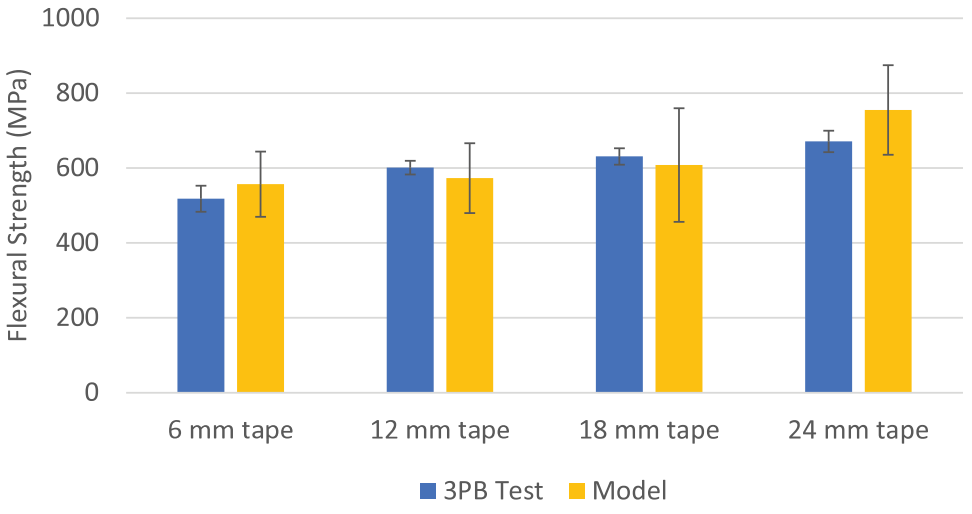


Figure 10. The effect of tape length on flexural strength under 3-point bending.

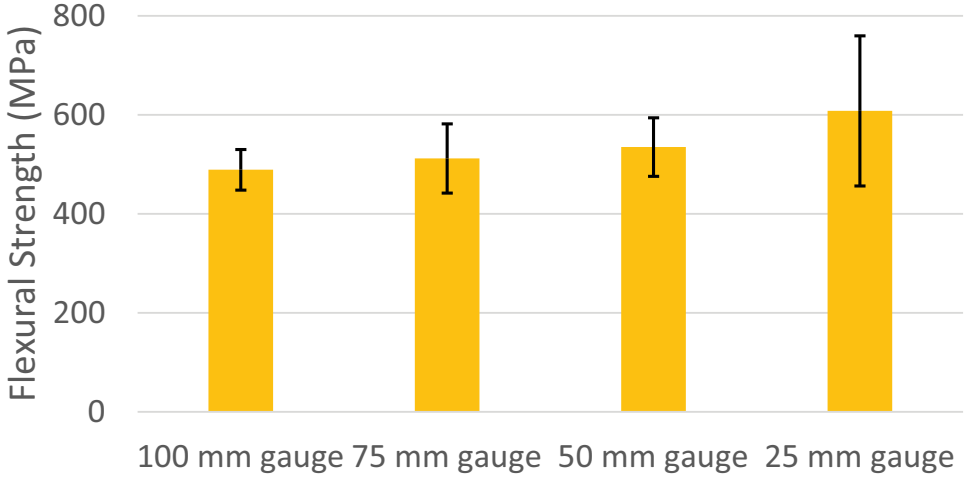


Figure 11. Scaling effect of predicted flexural strength and scatter.

weaker than expected. It can also be seen that the numerical scatter decreases with a larger gauge length or moulding area. This implies that a larger plate would fail more consistently, probably because the tape configuration is more uniform and fewer tapes are hanging outside the edges of the moulding area (Figure 4a). This could explain why the structures made of UT-ROS often perform more consistently than small specimens.

Scanning a greater range of angles of the critical tapes means a longer runtime, because more tapes need to be considered in Weibull criterion. The 10° angle results are used for comparison with the 4-point bending experimental data. Using 12

processors of one 12th Gen Intel® Core™ i7 -12,700 H 2.30 GHz CUP, the 10° angle run takes about 3 min for each tape configuration. It is much faster than the heterogeneous-particle model (about 2 h) when predicting the same UT-ROS material under 4-point bending with better CPUs [18]. When comparing against the detailed FE model, a single run of a model under tension can take over 4 h using one CPU [5]. In summary, the current stochastic model is very computationally efficient for structural applications.

Constant bending moment is a disadvantage of the current model e.g. when comparing to 3-point bending experiments. There is a need to combine the proposed stochastic model with FE analysis for structures subject to complex loading, potentially by using the current model as a surrogate model that generates strength and scatter for an FE model. This can be studied in an application in the future.

6. Conclusions

A stochastic modelling framework has been developed to predict flexural properties of Ultra-thin Randomly Oriented Strands (UT-ROS) of thermoplastic prepreg tapes. The model is suitable for UT-ROS material which exhibits fibre-dominant failures at the tension side under bending. The current modelling framework captures the average flexural modulus within 2.0% and average flexural strength within 1.1% under 4-point bending. Moreover, it also predicts the higher average flexural strength under 3-point bending (within 3.7%) than 4-point bending, and higher average flexural strength with longer tapes (up to 24 mm) under 3-point bending (within 12.5%). These agree with the new 3-point bending experimental results. The predicted scatter is however larger than the measured strength values in all cases, and a potential explanation is discussed in terms of moulded areas. The modelling framework is computationally efficient (within 31 min for 10 tape configurations) so potentially suitable for composite structures.

Acknowledgements

Xiaodong Xu would like to acknowledge valuable inputs of Dr Xin Zhang, Mr Zihao Zhao, Mr Ruochen Xu, Ms Qian Gao, and Mr Xiaohang Tong from the University of Tokyo. The work was financially supported by the Royal Society (IEC\R3\213017).

Disclosure statement

No potential conflict of interest was reported by the author(s).

Funding

The work was supported by the Royal Society [IEC\R3\213017].

ORCID

Xiaodong Xu http://orcid.org/0000-0003-1732-9323
André Jesus http://orcid.org/0000-0002-5194-3469

Data availability statement

The raw/processed data required to reproduce these findings cannot be shared at this time as the data also forms part of an ongoing study.

References

[1] Ishikawa T, Amaoka K, Masubuchi Y, et al. Overview of automotive structural composites technology developments in Japan. Compos Sci Technol. 2018;155:221–246. doi: 10.1016/j.compscitech.2017.09.015

[2] Almushaikeh AM, Alaswad SO, Alsuhybani MS, et al. Manufacturing of carbon fiber reinforced thermoplastics and its recovery of carbon fiber: a review. Polym Test. 2023;122:108029. doi: 10.1016/j.polymertesting.2023.108029

[3] Visweswaraiah SB, Selezneva M, Lessard L, et al. Mechanical characterisation and modelling of randomly oriented strand architecture and their hybrids – a general review. J Reinf Plast Compos. 2018;37(8):548–580. doi: 10.1177/0731684418754360

[4] Li Y, Pimenta S, Singgih J, et al. Experimental investigation of randomly-oriented tow-based discontinuous composites and their equivalent laminates. Compos Part A Appl Sci Manuf. 2017;102:64–75. doi: 10.1016/j.compositesa.2017.06.031

[5] Harper L, Qian C, Luchoo R, et al. 3D geometric modelling of discontinuous fibre composites using a force-directed algorithm. J Compos Mater. 2017;51(17):2389–2406. doi: 10.1177/0021998316672722

[6] Kravchenko SG, Sommer DE, Denos BR, et al. Tensile properties of a stochastic prepreg platelet molded composite. Compos Part A Appl Sci Manuf. 2019;124:105507. doi: 10.1016/j.compositesa.2019.105507

[7] Sattar S, Laredo BB, Kravchenko SG, et al. Effect of platelet length and stochastic morphology on flexural behavior of prepreg platelet molded composites. Polym Compos. 2023;44:2122–2137. doi: 10.1002/pc.27230

[8] Shah SZH, Choudhry RS, Mahadzir S. A new approach for strength and stiffness prediction of discontinuous fibre reinforced composites (DFC). Compos B Eng. 2020;183:107676. doi: 10.1016/j.compositesb.2019.107676

[9] Wan Y, Takahashi J. Tensile and compressive properties of chopped carbon fiber tapes reinforced thermoplastics with different fiber lengths and molding pressures. Compos Part A Appl Sci Manuf. 2016;87:271–281. doi: 10.1016/j.compositesa.2016.05.005

[10] Katsivalis I, Persson M, Johansen M, et al. Strength analysis and failure prediction of thin tow-based discontinuous composites. Compos Sci Technol. 2024;245:110342. doi: 10.1016/j.compscitech.2023.110342

[11] Galos J. Thin-ply composite laminates: a review. Compos Struct. 2020;236:111920. doi: 10.1016/j.compstruct.2020.111920

[12] Yamashita S, Hashimoto K, Suganuma H, et al. Experimental characterization of the tensile failure mode of ultra-thin chopped carbon fiber tape-reinforced thermoplastics. J Reinf Plast Compos. 2016;35(18):1342–1352. doi: 10.1177/0731684416651134

[13] Nakashima Y, Suganuma H, Yamashita S, et al. Influence of strand dispersion method on mechanical properties of randomly orientated carbon fibre strand thermoplastic composites. In: 21st International Conference on Composite Materials; Xi'an, China; 2017.

[14] Nakashima Y, Yamashita S, Zhang X, et al. Analytical modelling of the behaviour and scatter of the flexural modulus of randomly oriented carbon fibre strand thermoplastic composites. Compos Struct. 2017;178:217–224. doi: 10.1016/j.compstruct.2017.07.006

[15] Wan Y, Yamashita S, Takahashi J. Evaluation and modeling of tensile properties of chopped carbon fiber tapes reinforced thermoplastics of different tape thicknesses. Mech Compos Mater. 2022;58(3):395–408. doi: 10.1007/s11029-022-10037-y

[16] Wan Y, Zhang X, Sato Y, et al. Stochasticity modeling and analysis of elastic modulus of randomly oriented strands. Adv Compos Mater. 2021;30:286–306. doi: 10.1080/09243046.2020.1821467

[17] Jesus A, Xu X. Rapid prediction of fibre-dominant tensile failure in randomly oriented strands. J Reinf Plast Compos. 2023;42(5–6):205–212. doi: 10.1177/07316844221107927

[18] Qu P, Wan Y, Fang G, et al. A novel heterogeneous-particle model based on peridynamics for flexural mechanical properties of randomly oriented fiber reinforced composites. Compos B Eng. 2022;243:110140. doi: 10.1016/j.compositesb.2022.110140

[19] Weibull W. A statistical distribution function of wide applicability [internet]. J Appl Mech. 1951;18(3):293–297. Available from: http://web.cecs.pdx.edu/~cgshirl/Documents/Weibull-ASME-Paper-1951.pdf

[20] Li X, Hallett SR, Wisnom MR. Numerical investigation of progressive damage and the effect of layup in overheight compact tension tests. Compos Part A Appl Sci Manuf. 2012;43 (11):2137–2150. doi: 10.1016/j.compositesa.2012.03.002

[21] Li X, Hallett SR, Wisnom MR. A finite element based statistical model for progressive tensile fibre failure in composite laminates. Compos B Eng. 2013;45:433–439.doi: 10.1016/j.compositesb.2012.08.001

[22] Xu X, Wisnom MR, Li X, et al. A numerical investigation into size effects in centre-notched quasi-isotropic carbon/epoxy laminates. Compos Sci Technol. 2015;111:32–39. doi: 10.1016/j.compscitech.2015.03.001

[23] Xu X, Wisnom MR, Hallett SR. Deducing the R-curve for trans-laminar fracture from a virtual Over-height Compact Tension (OCT) test. Compos Part A Appl Sci Manuf. 2019;118:162–170. doi: 10.1016/j.compositesa.2018.12.027

[24] Reiner J, Xu X, Zobeiry N, et al. Virtual characterization of nonlocal continuum damage model parameters using a high fidelity finite element model. Compos Struct. 2021;256:113073. doi: 10.1016/j.compstruct.2020.113073

[25] IQBAL S, XIAO X, LI B, et al. Considering the randomness of mechanical properties in simulations of discontinuous fiber reinforced composites. In: American Society for Composites 2020; Lancaster, PA: DEStech Publications, Inc.; 2020.

[26] Selezneva M, Roy S, Lessard L, et al. Analytical model for prediction of strength and fracture paths characteristic to randomly oriented strand (ROS) composites. Compos B Eng. 2016;96:103–111. doi: 10.1016/j.compositesb.2016.04.017

[27] Wan Y, Suganuma H, Takahashi J. Effects of fabrication processes and tape thickness on tensile properties of chopped carbon fiber tape reinforced thermoplastics. Compos Commun. 2020;22:100434. Available from: https://www.sciencedirect.com/science/article/pii/S2452213920301625



https://dspace.org/

A stochastic modelling framework for predicting flexural properties of ultra-thin randomly oriented strands

Xu, Xiaodong; Jesus, André; Wan, Yi; Takahashi, Jun

2025-01-31
Taylor & Francis
https://doi.org/10.1080/09243046.2024.2351667
Xu X, Jesus A, Wan Y, Takahashi J. (2025) A stochastic modelling framework for predicting flexural properties of ultra-thin randomly oriented strands. Advanced Composite Materials, Volume 34, Issue 1, January 2025, pp. 1-15

Downloaded from a DSpace repository. https://dspace.org/